

## Chapter 2

# Parametric Signal Amplification in Continuous Time Domain

### 2.1 Introduction

Preceding the availability of high frequency, high gain and sufficiently low noise semiconductor transistors, the need to increase the radio receiver sensitivity as led to a concerted work among several research teams during the mid-fifties, [50]. One of the objectives was to reduce the impact of the signal loss and noise added at the mixing stages. To achieve this goal, LNAs were developed, designed and inserted between the antenna and the mixer stage of a conventional receiver architecture. As a result, the equivalent receiver noise temperature, during that period, has reduced from 3,000 to 1,000 K when using traveling-wave tube, or to 10 K in the case of a MASER, [50,51].

An alternative technique, which gained great popularity at that time, consisted on the implementation of parametric amplifiers (PAMP). The parametric amplifier operates through a nonlinear process of mixing and frequency conversion in a nonlinear reactance. Despite some ferrite based (inductor like) amplifiers were presented, the most used mixing reactance was the nonlinear variable capacitor (varactor). Since the process of amplification is based on the capacitance parameter change over time, rather than a transresistive/transconductance approach, it was expected to achieve very low noise level during the amplification step.

Nowadays, there are not many cases exemplifying the CMOS implementation of such parametric based circuits, despite the fact it is a well suited technology to implement varactors. This is justified by the continuous evolution of the MOS transistor, which has boosted the design of transconductance based signal amplifiers, which are fully and easily integrable on a chip. However, with the degradation of the transistor intrinsic gain due to the continuous CMOS scaling, described in Chap. 1, the parametric amplifier alternative technique is recovering some interest, particularly in the microwave domain.

This chapter is dedicated to the review of the continuous time parametric signal processing applied to signal amplification and frequency conversion. Also a short reference is done on the application of this technique in traveling wave amplifiers.

Targeting design of parametric amplifiers in CMOS technology, an introduction of the available MOS varactor configurations is given. After this preliminary study on the continuous time parametric amplification, Chap. 3 extends the analysis towards the discrete-time version of this technique.

## 2.2 Using a Reactance to Build a Transistor-Free Amplifier

In a transistor based amplifier, the flow of additional energy delivered to the load, which is needed to achieve a power gain higher than one, is supplied from a DC power source. In simplistic terms, the input signal modulates the injection of energy coming from the DC power supply towards the load by means of a transconductance operation. This feature of the transistor is usually (at least in the MOS case) dependent on the DC biasing current and thus impacting both, efficiency and power dissipation. Additionally, if one recognizes that a resistive and, therefore, a dissipative property is intrinsically embedded into this amplification process, a non negligible thermal noise component has to be taken into account.

Interestingly, the delivery of energy to the load does not need to be performed directly from the DC power supply but, instead, can be transferred from an AC power source. Instead of a resistive (conductance) and dissipative element, a non-linear energy storage element can be used to perform this energy transfer. One advantage that seems to emerge in first place is the fact that the amplifier output thermal noise can be significantly reduced by using a low-loss reactance (in theory, a noise free amplification process could be achieved with an ideal lossless reactance). The amplifier built around a reactance element is usually referred as a parametric amplifier (PAMP) since its operation relies on the controlled time variation of a reactance parameter. When using a nonlinear capacitor the variable parameter is the capacitance value (the same applies for the inductance property of an inductor).

To achieve power gain from this parametric type network one must follow the condition set in [52] or [53], which states that a necessary condition to achieve power amplification from a nonlinear network, whose individual elements are passive, is the use of one nonlinear reactive device and one AC power source. A classical approach to explain the operation of a parametric amplifier is to analyze the energy balance of a capacitor excited by an electrical time varying signal and simultaneously by a mechanical periodic “pump” force, as shown in Fig. 2.1. The “pump” force is applied to change the distance,  $y$ , between the capacitor plates (thus changing the capacitance value). Applying the analysis from [54], when in presence of a time variation on the capacitance,  $C(t)$ , it can be shown that the instantaneous charge stored in the capacitor  $q(t)$ , represented in Fig. 2.1, is given by

$$q(t) = C(t) \cdot v(t), \quad (2.1)$$

where  $v(t)$  is the total voltage applied to the plates of the capacitor. Besides the usual capacitive current generated by  $v(t)$ , the total current,  $i(t)$ , through the capacitor also

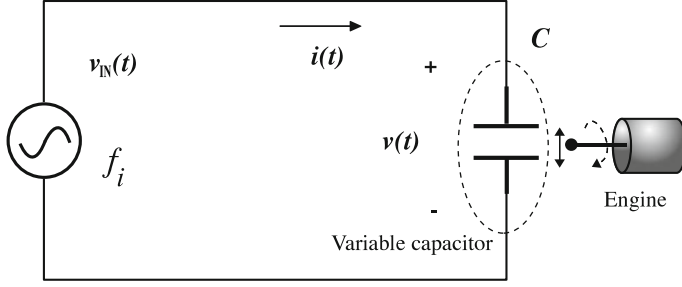


**Fig. 2.1** Simple model for the parametric capacitor

reflects the variation of the capacitance created by the mechanical operation of the virtual/imaginary engine since

$$i(t) = \frac{dq(t)}{dt}. \quad (2.2)$$

As usual, the energy stored in the electrical field is given by

$$W_{cap}(q, C) = \frac{1}{2} \cdot \frac{q^2}{C}. \quad (2.3)$$

Under these conditions, the total energy stored in the capacitor can be determined by applying the derivate chain rule to (2.3),

$$P_{cap} = \frac{dW_{cap}}{dt} = \left( \frac{\partial W_{cap}}{\partial q} \right)_C \frac{dq}{dt} + \left( \frac{\partial W_{cap}}{\partial C} \right)_q \frac{dC}{dt}, \quad (2.4)$$

resulting in

$$P_{cap} = \frac{q}{C} \cdot i + \left( \frac{\partial W_{cap}}{\partial C} \right)_q \frac{dC}{dy} \cdot \frac{dy}{dt} = v \cdot i + \underbrace{\left( \frac{\partial W_{cap}}{\partial y} \right)_q}_{\text{force}} \underbrace{\frac{dy}{dt}}_{\text{velocity}}. \quad (2.5)$$

A deeper analysis of (2.5) reveals that the first part of the equation represents the electrical power resulting from  $v(t)$  while the renaming one reflects the mechanical power transferred from the external imaginary engine,

$$P_{cap} = \underbrace{P_{e,v}}_{\text{due to } v(t)} + \underbrace{P_m}_{\text{mechanical}}. \quad (2.6)$$

Furthermore, this result indicates that the capacitor can be used as an energy converter between different domains or, as it will be shown in Sect. 2.4, between signals with different frequency. This is in fact the basis of the parametric operation, where the capacitor is used as an active element.

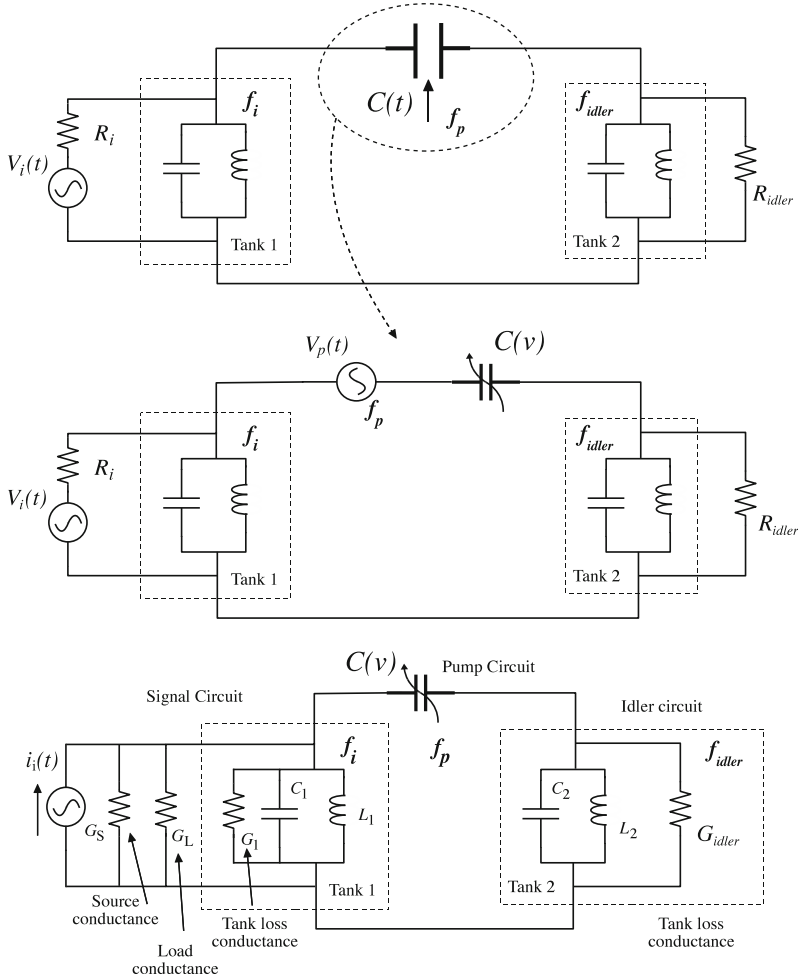


**Fig. 2.2** Equivalent model for a two-tank parametric amplifier

To transpose the initial schematic into a more practical and fully electrical circuit, one must find a way to electrically change the capacitance value instead of doing it by mechanical means. Such operation can be reached through the use of a modified capacitor that reacts non-linearly with respect to the applied voltage. The resulting mixing effect that occurs in the nonlinear capacitor permits an energy transfer and a frequency combination between a weak signal (e.g., coming from an RF antenna) and a relatively strong pump source (e.g., a local oscillator). Both signals are superimposed across the nonlinear capacitor, see Fig. 2.2. The mixing that occurs between the input signal  $v_i(t)$  with frequency  $f_i$  and the pump source  $v_p(t)$  with frequency  $f_p$  generates a set of harmonics with frequencies located at

$f_0 = m f_p \pm n f_i$ . Usually only one of them is somehow extracted from the circuit. The following analysis assumes that the output signal corresponds to the harmonic with frequency  $f_0 = f_p \pm f_i$ . A generalized result is presented in Sect. 2.4.

When using a nonlinear capacitor, the charge  $q(v)$  is also a nonlinear function of the applied voltage  $v(t)$  and therefore may be expanded in a Taylor series given by

$$q(v) = \alpha_1 v + \alpha_2 v^2 + \alpha_3 v^3 + \dots \quad (2.7)$$

Considering only the first two terms of (2.7), as long as the voltage across the capacitor is not too large [55], the current flowing in the nonlinear capacitance is obtained from

$$i(t) = \frac{dq(t)}{dt} = \underbrace{\alpha_1}_{C_0} \frac{dv(t)}{dt} + \underbrace{2\alpha_2 v(t)}_{C_v(t)} \frac{dv(t)}{dt} = (C_0 + C_v(t)) \frac{dv(t)}{dt} \quad (2.8)$$

The result from (2.8) confirms that, if properly driven by a pump signal, the nonlinear capacitor behaves like a time-varying linear capacitance thus validating its use in a parametric circuit configuration.

Figure 2.2 represents a possible configuration for a parametric amplifier based on a nonlinear capacitor  $C$  whose capacitance value is changed by a pump signal of frequency  $f_p$ . Associated with the input signal with frequency  $f_i$  is a circuit tank consisting of  $L_1$ ,  $C_1$  and  $G_{t1} = G_S + G_L + G_1$  represents the total loading due to source, load resistance and internal tank losses. Similarly, the sideband frequency  $f_{idler}$  has an associated resonant tank circuit formed by  $L_2$ ,  $C_2$  and  $G_{idler}$ .

Depending on the relation between the three involved frequencies, the circuit has slightly different designations, [56]:

- Negative-Resistance Amplifier, if the output frequency is the same as the input one.
- Down-Converter Amplifier, if the output signal frequency (taken from the idler tank) is the difference between the pump and input signal frequencies, i.e.,  $f_{idler} = f_i - f_p$ .
- Up-Converter Amplifier, if the output signal frequency (taken from the idler tank) is the sum between the pump and input signal frequencies, i.e.,  $f_{idler} = f_i + f_p$ .

As indicated above, if the upper sideband is filtered out, and the output is taken at the input signal frequency, then a negative resistance parametric based amplifier is built. In this case, the output signal is physically extracted from the circuit at the input tank. The remaining part, formed by the second tank plus the nonlinear capacitor, behaves as a negative resistance which is responsible for the amplifying operation of this “reflection” type of amplifier. From [55] and [56], the negative conductance is given by

$$G = \frac{\omega_i \omega_{idler} C^2}{4 G_{idler}} \quad (2.9)$$

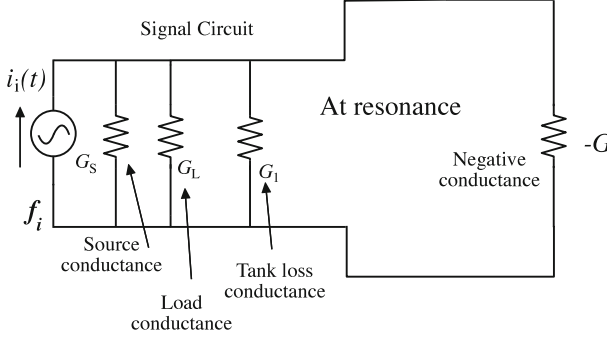


**Fig. 2.3** Equivalent model for a two-tank parametric amplifier at resonance

where  $\omega_{idler} = 2\pi f_{idler} = \omega_p - \omega_i$ , and the remaining parameters have already been defined. The power gain corresponds to the ratio of the power dissipated in the load conductance  $G_L$  to the available power from the input signal source with conductance  $G_S$ . Using the negative conductance calculated in (2.9), the power gain at resonance is determined by

$$G_{pwr} = \frac{4G_S G_L}{(G_{t1} - G)^2} \quad (2.10)$$

where  $G_S$  and  $G_L$  are the loading effect due to the input source and output load, respectively. Both are calculated at the frequency of the input signal. Additionally, (2.10) demonstrates that an oscillating regime is possible and occurs when  $G = G_{t1}$ .

The  $F$  of the negative resistance amplifier can be determined from the ratio between the output and input SNR. To calculate  $F$  at resonance state, the circuit model represented in Fig. 2.3 can be used.

$$F = \frac{1}{G_{pwr}} \cdot \frac{1}{kTB} \cdot N_o = \frac{1}{4kTB} \cdot \frac{(G_{t1} - G)^2}{G_S G_L} \cdot N_o \quad (2.11)$$

In (2.11),  $B$  is the bandwidth,  $T$  is the noise temperature in Kelvin,  $k$  the Boltzmann's constant,  $N_o$  is the total output referred noise, and the remaining parameters have already been defined. A detailed analysis is done in [56], in which all noise sources were added at the output, thus resulting in the closed expression given by

$$F \approx 1 + \frac{G_1}{G_S} + \frac{G}{G_S} \frac{f_i}{f_{idler}}. \quad (2.12)$$

Remarkably from (2.12), the lowest possible  $F$  obtainable is equal to  $1 + f_i/f_{idler}$ . Therefore, the use of an higher difference frequency  $f_{idler} = f_p - f_i$  contributes to lower  $F$ .

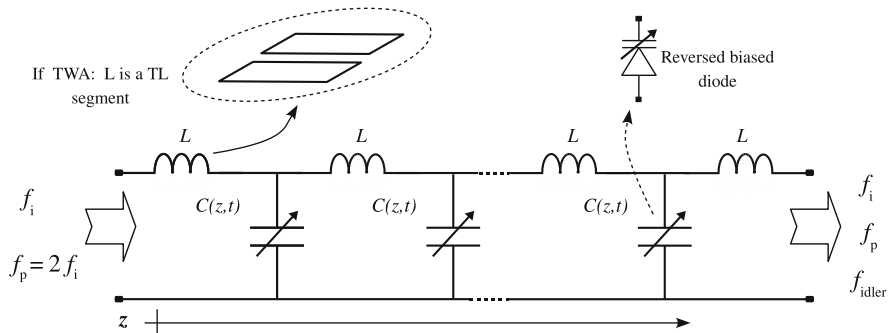


**Fig. 2.4** Model for a traveling wave parametric amplifier

Several configurations were used in the past to implement parametric amplifiers. Despite some reported amplifiers were based on ferrite/ferromagnetic (as the variable reactance), [57], the use of semiconductor solid-state diode was definitively the primary choice when designing a parametric amplifier at that time, [50]. In fact, in the former case the amplifier needed a large pump power while with the varactor diode case the requirements for the pump power are less stringent. The utilization of diode varactor also permitted the construction of more “compact” and less costly amplifier that could achieve low  $F$  even at room temperature. The effective noise temperature of a parametric diode based amplifier could be as low as 30 or 50 K (corresponding to a 1.3 dB Noise Factor), [57]. It was used in several applications. (e.g., military radars) ranging from 200 MHz to 35 GHz operation frequency and achieving a single stage gain ranging from 5 to 20 dB, [51, 58–60].

Up to now, the described parametric amplifier uses only a single variable reactance element and one or more resonant circuits. With this configuration, it is possible to obtain a reasonable gain with small Noise Figure footprint. Nevertheless, the use of high  $Q$  tanks squeeze the amplifier bandwidth [61]. An alternative for the parametric amplifier construction utilizes a distributed approach, being the traveling-wave structure one of the most important, [54, 61–65]. In this type of structure, several varactors are distributed along a propagating wave circuit (e.g., transmission line), contributing each one of them with a small amount of signal gain. Amplification of the signal power is then obtained in the form of a growing wave propagating along this structure of shunt varactors separated by series of inductances or transmission line sections. A general distributed amplifier model is shown in Fig. 2.4. When the lumped inductors of a distributed amplifier are replaced by transmission lines, the new circuit configuration is generally designated by Traveling Wave Amplifier (TWA), [66].

In Fig. 2.4, the variable capacitors  $C(z,t)$  are varactors (e.g., reversed biased diodes) whose capacitance is a function of position and time. The capacitance depends on its position since the amplifier acts as a terminated transmission line when considering the wavelength of the pump signal. The operation is supported on two propagating modes. One mode is excited by the input signal and, the other

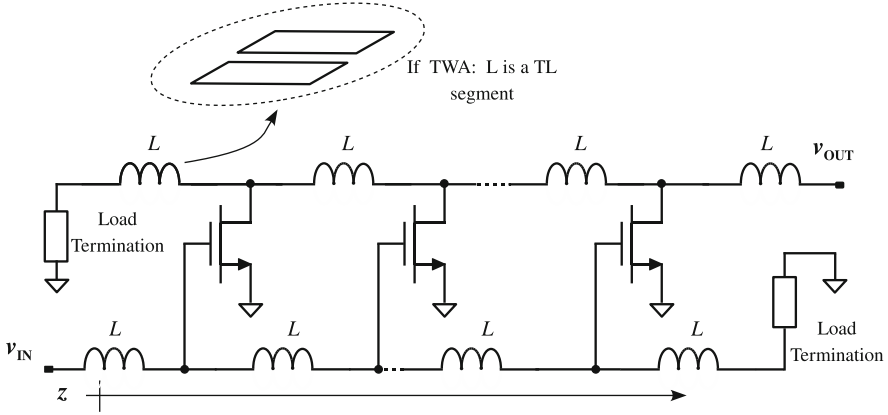


**Fig. 2.5** Simplified model of a MOSFET distributed amplifier

mode is used as the idling circuit. Additionally, the structure processes the traveling wave generated by the pump signal which provides, by modulating the capacitance of the varactors, a time varying coupling between the two propagating modes. This coupling behavior originates the necessary AC energy transfer for the parametric amplification to work. One of the first implementations of a TWA [64] using varactor diodes achieved more than 10 dB of gain, a noise temperature of 74 K (NF of 1.9 dB), 100 MHz of bandwidth, with a 10 mW pump signal at 890 MHz. Similar results were obtained in [54, 61, 65].

Distributed amplifiers have been already integrated in CMOS technology [66–68]. A simplified schematic of the usual reported approach is depicted in Fig. 2.5. As shown in Fig. 2.5, the MOS devices, that are separated by inductors or transmission line (TL) segments, are used in a common source configuration. The drains and sources are connected by a two separated TL. The original signal is fed into the input TL. Each gate is then affected by it as it will propagate along the line until it reaches the matched termination. At the drain a current is correspondingly injected into the output TL. If the phase constant of both lines are similar, it is expected that these drain currents add constructively at the output, [66]. A recent implementation of a 7 stage structure CMOS TWA, [68], in a standard 130 nm CMOS digital technology, achieved 8.5 dB of gain up to 40 GHz, a 3 dB bandwidth of more than 50 GHz and a Noise Figure below 7 dB.

The use of MOS varactors in TWA is not common. However, to reduce the Noise Figure, a slightly modification can be made in the circuit of Fig. 2.5 which consists on replacing the active conductance transistors by MOS varactors, which are energized by a common pump oscillator.



## 2.3 Varactors in CMOS Technology

By the time the parametric amplifier was strongly developed, the semiconductor diode played an important role as a simple and nonlinear variable capacitor element. This component continues to be available today, namely, within most of the standard CMOS generations and therefore a short description is given next.

Creating a junction between a P-type and N-type doped regions in a Silicon (Si) environment, [69] originates a distinct electronic element. The resulting diode semiconductor has a nonlinear operation, which results from the balance between a few physical phenomenons that appear across the junction. The most important ones are diffusion of carriers and the corresponding and opposite built-in electric field, [29].

By applying an external voltage higher than a threshold voltage, the mobile carriers gain sufficient momentum to cross the junction barrier thus creating the necessary conditions for electrical current to flow. The diode is said to be in a forward biased state.

In the opposite case, a negative voltage is applied to the PN junction, putting the diode in reverse-biasing condition in which a negligible DC current flows. This is due to the extension of the depletion region that surrounds the junction interface. Inside the depleted region, the majority mobile carrier are a scarce resources (all of them where moved apart by the external electrical field). Under these conditions, the P-type and N-type regions behave like capacitor plates while the depletion region acts as the “dielectric” between them. The thickness of this depletion region defines the distance between the capacitor plates, directly affecting the equivalent capacitance value. Knowing the depletion region length,  $d_j$ , one can determine the equivalent small signal capacitance value of the reverse biased diode, [29], resulting in

$$C_j(V_R) = \frac{\epsilon_{si} A}{d_j} = \frac{A \cdot \sqrt{2q\epsilon_{si} \frac{N_A N_D}{N_A + N_D}}}{2\sqrt{V_R + \phi_{bi}}} = \frac{C_{j0}}{\left[1 + \frac{V_R}{\phi_{bi}}\right]^{\alpha_j}}, \quad (2.13)$$

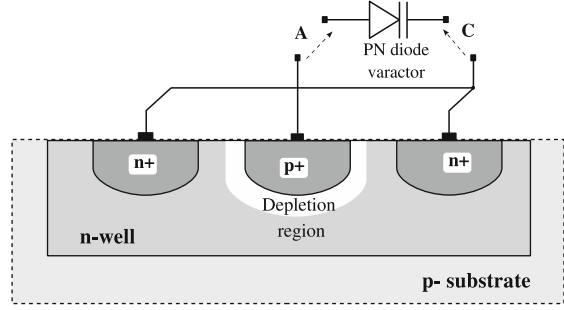
where  $A$  the junction cross-sectional area,  $N_A$  and  $N_D$  are the acceptor and donor densities,  $\phi_{bi}$  is the built-in potential of the junction (given by the difference between the Fermi potentials of the N and P sides, [29]),  $C_{j0}$  denotes the capacitance value for zero reverse diode voltage  $V_R$ . The value of  $\alpha_j$  reflects the doping profile which is equal to  $1/2$  for an abrupt one and  $1/3$  for a linearly graded junction.

The obtained result (2.13) reveals that the reversed biased diode capacitance is a nonlinear function of the applied voltage thereby validating its use in a continuous time parametric amplification.

To characterize the varactor performance, a few specifications have been defined. One of them reflects the capacitance tuning range of the device and is usually described by the ratio between the maximum and minimum capacitance values,

$$C_r = \frac{C_{max}}{C_{min}}. \quad (2.14)$$

**Fig. 2.6** P+ to n-well diode based varactor



Another important figure of merit to measure the varactor operation is the quality factor, [70], defined by

$$Q = 2\pi \frac{\text{Stored energy}}{\text{Dissipated energy per cycle}} = \frac{1}{\omega RC}, \quad (2.15)$$

where  $R$  and  $C$  are the values of the series resistance (loss) and capacitance.

Varactor based on junction diodes can be used in standard CMOS technology, but here only source/drain to well junctions are available. An example of diode structure is depicted in Fig. 2.6. Another configurations are possible and can be seen in [70]. This type of PN diode can reach high quality factor (higher than 20) when implemented in MOS technology, [71, 72], but the tuning range is small, lower than 2, [72]. Furthermore, since the charge *versus* voltage (C-V) diode characteristic is not very sharp, the tuning range tends to worsen due to MOS technology downscaling and to the decrease of the voltage dynamic range. Alternatively one can use two type of integrated MOS varactors: an Accumulation mode MOS varactor (AMOS) and an Inversion mode MOS varactor (IMOS).

In a P-type substrate MOS technology, the accumulation NMOS varactor (ANMOS), shown in Fig. 2.7, is implemented in a N-well region. The controlling varactor voltage is applied between the drain/source N+ implants areas and the other varactor terminal, the gate. The variation of the capacitance set by the controlling voltage is obtained by changing the state of the device from accumulation to depletion and vice-versa. When in depletion the total gate capacitance is given by the series of the oxide capacitance  $C_{ox}$  and the depletion capacitance  $C_{dep}$ , resulting in a small value (due to  $C_{dep}$ ). On the opposite direction, the varactor reach a maximum value of  $C_{ox}$  when in deep accumulation state. Despite the sharper C-V characteristic when compared with the diode based varactor, the accumulation mode varactor also suffers from the reduced control voltage range imposed by the advanced CMOS technology nodes. In fact, the C-V sharpness, for accumulation MOS varactor, is not sufficiently high to maximize the tuning range in case of controlling voltage lower than 1 V, [73].

It can be observed in the C-V characteristic of a MOS transistor configuration that, the transition between depletion to inversion is much faster than from depletion into accumulation. This is due to the distinct physical phenomena that happens

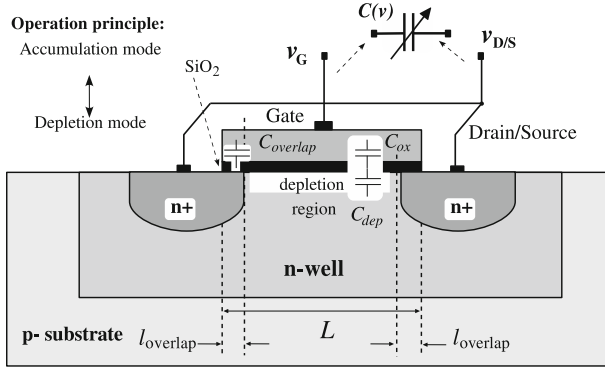


Fig. 2.7 Accumulation mode MOS varactor

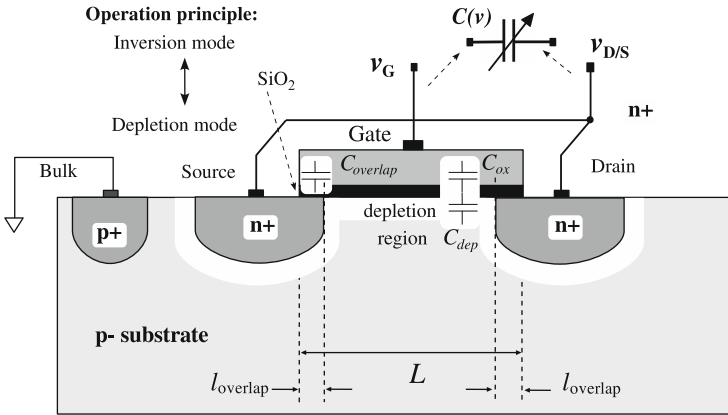


Fig. 2.8 Inversion mode MOS varactor

in each case. When the MOS device enters in weak inversion region, the fast capacitance change towards  $C_{ox}$  is due to the exponential growth of the charge at the interface Si-SiO<sub>2</sub> (corresponding to the channel below the gate area). In order to facilitate the use  $C-V$  characteristic segment from depletion to inversion, a simpler configuration based on a standard MOS transistor can be adapted. In fact, it is just needed to setting up a short-circuit between the drain and source and designate the gate terminal as the other capacitor plate. Figure 2.8 illustrates the resulting Inversion Mode MOS varactor (IMOS), implemented from a NMOS device.

The variation in capacitance is greater in inversion and accumulation MOS varactor than in PN junction type. Consequently, higher tuning range is achievable with the former type, considering the same device area. With respect to the quality factor, the PN type varactor reaches better values due to their lower resistance, [70]. The higher losses in the MOS varactor compared to PN-junction varactor come partly from the ohmic loss of the polysilicon gate, partly from the high series

**Table 2.1** Performance comparison between varactor in MOS technology, [72]

Varactor type	$C_{max}/C_{min}$	$Q_{min}$	$Q_{max}$
Diode (p <sup>+</sup> to n-well)	1.32	18.0	22.6
Diode (p <sup>+</sup> to n-well, small size)	1.23	94.5	109.0
Accumulation NMOS	1.69	33.2	38.3
Inversion NMOS	2.15	25.8	34.3

resistance of the lightly-doped area near the source and drain regions, and also from the channel conductance (when in inversion state), [74, 75]. Nevertheless, MOS varactors are much more area-efficient (in terms of absolute capacitance values) and show much sharper C-V characteristics, which is very important for low voltage applications, [73]. Additional degradation from parasitic factors contributes to the lower the quality factor of the MOS varactor as losses in the substrate and the well, the ohmic losses of metal and polysilicon interconnections, and the parasitic capacitances, [70, 72].

Reference [72] presents a comparative analysis between the three varactor structures, based on experimental results obtained from an old 0.5  $\mu\text{m}$  CMOS technology. Table 2.1 summarizes the experimental reported results. Results for more recent technologies, [70, 73, 76, 77] show similar trends.

Inversion MOS-based varactors are gaining more interest over the reverse-biased diodes due to their wider tuning range and lower voltage range of operation, both of which improve with every new process generation. In particular, the discrete-time amplification technique that is used throughout this work, uses an inversion based MOS varactor as the parametric reactance device.

## 2.4 Manley–Rowe Power Relations for Nonlinear Reactances

Only several year later from its initial work, [50], Jack Manley and Harrison Rowe have finished the development of a number of fundamental equations concerning the flow of energy between the different signals frequencies components originated when a nonlinear and lossless reactance is driven by distinct signals simultaneously. The power relations between these signals are described by the designated Manley–Rowe relations, [78, 79].

When applying simultaneously a strong local oscillator, or pump signal, of frequency  $f_p$  and an input signal of  $f_i$  to a nonlinear capacitor, the set of new frequencies that will appear in the circuit includes harmonic, sum and difference combinations in the form of  $f_{m,n} = mf_p + nf_i$ , with  $m$  and  $n$  integer positive, negative, or zero. Additionally, the two fundamental frequencies  $f_p$  and  $f_i$  are considered to be positive and incommensurable (leading to independent variables) [78] and the other ones are the resulting sidebands.

The determination of the power relations is based on the analytical model represented in Fig. 2.9, where resistive loads are connected in series with an ideal bandpass filter. Each resistive branch is then connected in parallel to the nonlinear

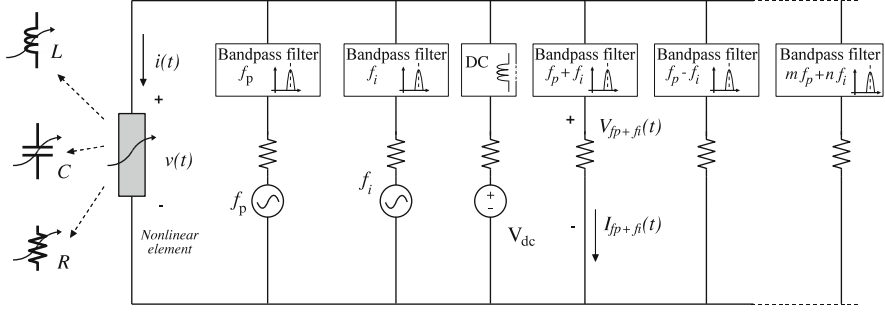


Fig. 2.9 Circuit model for the Manley–Rowe relations

capacitor. As mentioned before, it is assumed that the nonlinear element is lossless and does not present any hysteresis in the characteristic charge-voltage, C-V, in case of a capacitor, or inductance-current, L-I, in case of an inductor. Since the nonlinear capacitor is purely reactive, it does not dissipate energy, that is, no net power into or out of this element will be possible. In other words, the lossless nonlinear capacitor do store energy but it does not dissipate it. Adding the fact that the fundamental frequencies are considered to be incommensurable, the time-average power due to interacting harmonics will be null, [69]. In particular, the form taken by the principle of energy conservation in this case is expressed by

$$\sum_{n=-\infty}^{\infty} \sum_{m=-\infty}^{\infty} P_{nm} = 0, \quad (2.16)$$

where the sum extends to all signal frequencies generated at the nonlinear reactance.  $P_{nm}$  is the average power at frequency  $f_{m,n} = m f_p + n f_i$  and in the nonlinear reactance case, only the real power  $P_{nm}$  appears, [78].

$$P_{n,m} = V_{n,m} I_{n,m}^* + V_{n,m}^* I_{n,m} = 1/2 \operatorname{Re} [V_{n,m} I_{n,m}^*] \quad (2.17)$$

The  $I_{n,m}$  and  $V_{n,m}$  components in (2.17), are the coefficients of the double Fourier series associated to the total voltage and current present at the nonlinear reactance (a capacitor in this case), which are described in (2.18)–(2.20).

$$v = \sum_{n=-\infty}^{\infty} \sum_{m=-\infty}^{\infty} V_{n,m} e^{j(n\omega_p t + m\omega_i t)} \quad (2.18)$$

For signal  $v(t)$  to be real, one must satisfy  $V_{m,n} = V_{-m,-n}^*$  and  $V_{-m,-n} = V_{m,n}^*$ , for the complex amplitudes. The coefficients are given by

$$V_{n,m} = \frac{1}{4\pi^2} \int_0^{2\pi} dy \int_0^{2\pi} dx \cdot v \cdot e^{-j(nx+my)}, \quad (2.19)$$

where  $x = \omega_p t$  and  $y = \omega_i t$ . In the same way, the total current flowing in the capacitor can be expanded in double Taylor series as well, resulting in

$$\begin{aligned} i = \frac{dq}{dt} &= \sum_{n=-\infty}^{\infty} \sum_{m=-\infty}^{\infty} j(n\omega_p + m\omega_i) Q_{n,m} e^{j(n\omega_p t + m\omega_i t)} \\ &= \sum_{n=-\infty}^{\infty} \sum_{m=-\infty}^{\infty} I_{n,m} e^{j(n\omega_p t + m\omega_i t)}. \end{aligned} \quad (2.20)$$

Note that the current calculation in the capacitor has assumed a nonlinear function of the charge with respect to the applied voltage  $q = f(v)$ . Furthermore, it was assumed that this function meets all conditions, namely single-value, to be expanded in Taylor series. From (2.16) and after some manipulation, the Manley–Rowe relations are derived, [69, 78, 79], resulting in

$$\sum_{n=0}^{\infty} \sum_{m=-\infty}^{\infty} \frac{n P_{n,m}}{n\omega_p + n\omega_i} = 0 \quad (2.21)$$

$$\sum_{m=0}^{\infty} \sum_{n=-\infty}^{\infty} \frac{m P_{n,m}}{n\omega_p + n\omega_i} = 0 \quad (2.22)$$

where  $n$  and  $m$  are integers and  $P_{n,m}$  represents the power series coefficients. Although the condition of energy conservation (i.e., the varactor with no losses) is necessary for the previous derivation, it also depends on the long term averaged power of a component to be proportional to its frequency, [80]. The later condition occurs in the capacitor case, where the instantaneous power is given by the product of  $v$  and  $dq/dt = i$ . In fact when differentiating  $q$  with respect to time, the term becomes multiplied by the corresponding frequency  $n\omega_p + m\omega_i$ .

A general power relations for nonlinear resistive elements can be found in [81] and the extension for more than 2 exciting sources can be found in [80]. An example of using the Manley–Rowe results is the up-converter parametric circuit topology, where it is only allowed to flow the currents associated to  $f_i$ ,  $f_p$  and  $f_i + f_p$ . Using the results of (2.21) and (2.22), one can obtain the following relations between signal frequencies:

$$\frac{P_{1,0}}{\omega_i} + \frac{P_{1,1}}{\omega_i + \omega_p} = 0, \quad (2.23)$$

$$\frac{P_{0,1}}{\omega_p} + \frac{P_{1,1}}{\omega_i + \omega_p} = 0. \quad (2.24)$$

The supplied power is provided at frequencies  $f_i$  and  $f_p$ , which means that the  $P_{1,0}$  and  $P_{0,1}$  component power are positive. As a consequence the power at the sideband harmonic component is negative meaning that the power is delivered to the load from the nonlinear reactance at the frequency  $f_i + f_p$ . This results in the maximum achievable power gain given by

$$-\frac{P_{1,1}}{P_{1,0}} = \frac{f_p + f_i}{f_i} = 1 + \frac{f_p}{f_i}. \quad (2.25)$$

Similar relations can be obtained for downconverter parametric circuits or just parametric amplifiers (where  $f_{out} = f_i$ ), [69].

## 2.5 CMOS Parametric Amplification with Frequency Conversion in Continuous Time Domain

In a receiver chain, the frequency downconversion stage can be accomplished by a parametric based mixing circuit. Not only a reduced noise addition is expected from this operation (due to the low noise parametric characteristic) but, if the local oscillator frequency is conveniently chosen, the parametric mixer can also deliver an effective extra power gain. In fact, if one choose to use a local oscillator frequency  $f_p = f_{LO}$  higher than the RF carrier frequency  $f_i = f_c$  (but lower than  $2f_c$ ), from the Manley-Rowe expressions one could expect an effective conversion power gain implicitly described by (2.26) and (2.27). The negative power expressed in (2.27) means that the nonlinear reactance is delivering power to the IF load. The energy is coming from the local oscillator but to reach an IF power higher than the input signal, the power of the local oscillator must be higher than the one of the input signal.

$$P_{IF} = \frac{f_{IF}}{f_i} \cdot P_i \quad (2.26)$$

$$P_{IF} = -\frac{f_{IF}}{f_{LO}} \cdot P_{LO} \quad (2.27)$$

The Manley–Rowe relations establish a maximum limit of the power conversion gain under loss-less conditions and, interestingly, they depend on frequency relations rather than explicit circuit implementation details. However, to obtain the actual power gain expression, a two-port analysis can be adapted for the mixer case. To support this approach, a conversion matrix (admittance or impedance type) is filled up [69, 82, 83] under the conditions of strong LO signal (in comparison to the input RF signal). This reasonable requirement means that only the oscillator signal is responsible for the variations of the nonlinear reactance element. A complementary analysis based on a coupled-mode theory can be found in [83].

The mixer conversion matrix describes the relationships (and couplings) between voltages and currents, in a phasor type notation (assuming sinusoidal regime), coming from different circuit sections that operate at different frequencies, as shown in Fig. 2.10. Under this construction, one must also account for the losses due to the varactor. Considering the typical structure of a MOS varactor, a resistor  $R_s$  might be included in series with the variable reactance, [84]. Moreover, to represent the voltages at the varactor two-port model (including losses), it is better to represent the variable capacitor by its elastance rather than the capacitance [54, 84, 85]. Therefore,

$$v(t) = R_s \cdot i(t) + \int S(t) \cdot i(t) dt, \quad (2.28)$$

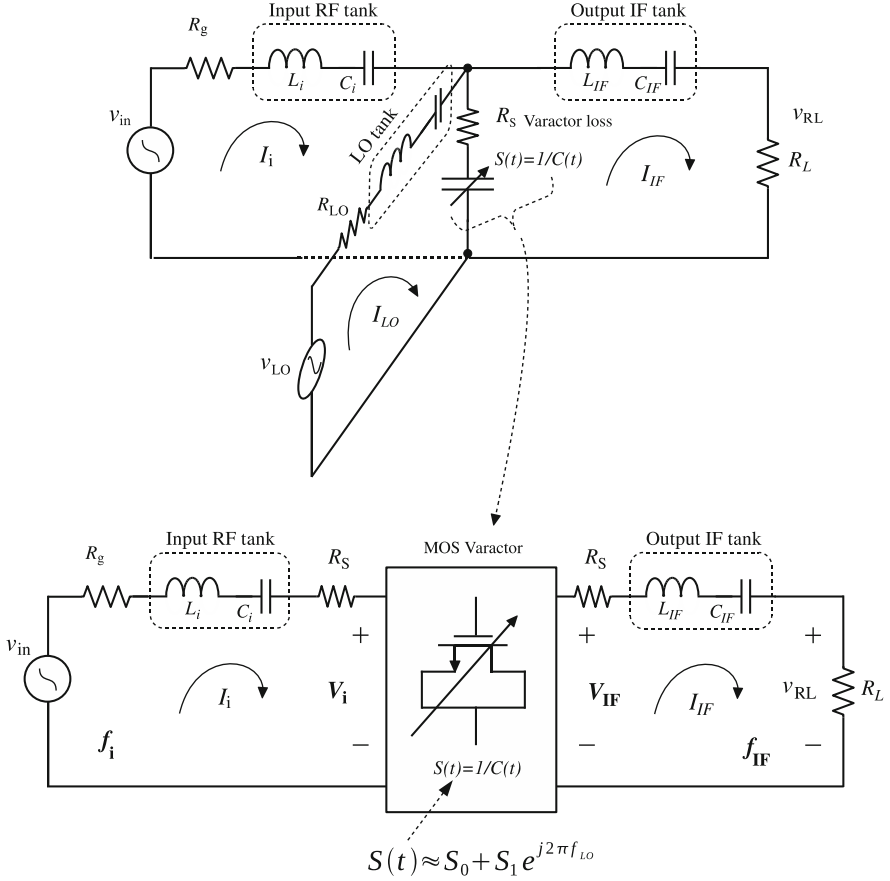


**Fig. 2.10** Equivalent simplified model for the parametric mixer

where  $S(t)$  represent the elastance of the varactor as a function of time,

$$S(t) = \frac{1}{C(t)} = \sum_{p=-\infty}^{+\infty} (S_p e^{jp\omega_{LO}t}). \quad (2.29)$$

Inside the mixer circuit three frequencies coexist and all the remaining ones are assumed that are filtered out by tuned LC tanks. These three frequencies include the input signal frequency  $f_i$ , the local oscillator  $f_{LO}$ , and the intermediate signal frequency  $f_{IF}$ . Moreover, it is considered that all of them are coupled together only through the time-varying component of the varactor. Therefore, the equivalent circuit model, when only the input and IF (output) sections are explicitly shown, is illustrated in Fig. 2.10.

Based on the previous model, the conversion impedance matrix, [83],

$$\begin{bmatrix} V_i \\ V_{IF}^* \end{bmatrix} = \begin{bmatrix} R_s + \frac{S_0}{j2\pi f_i} & -\frac{S_1}{j2\pi f_{IF}} \\ \frac{S_1^*}{j2\pi f_i} & R_s - \frac{S_0}{j2\pi f_{IF}} \end{bmatrix} \cdot \begin{bmatrix} I_i \\ I_{IF}^* \end{bmatrix}, \quad (2.30)$$



is obtained for the downconversion parametric mixer case where the local oscillator frequency is higher than the input RF signal frequency. This latter fact establishes a direct coupling to the negative intermediate frequency which is shown as conjugate voltages and currents phasors. In (2.30),  $S_0$  is the varactor average value while  $S_1$  represents the elastance variation at the LO frequency.

The conversion matrix reflects a linearization process applied around the non-linear varactor that involves currents and voltages at different mixing frequencies (which are coupled through the variable component of the varactor). Since, under these conditions, linear circuit theory holds true for each matrix element, Kirchoff's laws can be applied to connect the circuit elements thus originating closed form for the power conversion gain between RF and IF signals. Considering that the mixer is in a tuning state, the midband conversion power gain is determined from the output power developed in  $R_L$ ,  $\frac{1}{2} |I_{IF}|^2 R_L$ , and from the available power at input,  $V_{in}^2 / 8R_g$ . The final result of the gain at IF, [83, 86], is given by

$$G_{IF} = \frac{4 \cdot R_L R_g \cdot |S_1|^2}{\left[ 2\pi f_i \cdot (R_L + R_s) (R_g + R_s) - \frac{|S_1|^2}{2\pi f_{IF}} \right]^2}, \quad (2.31)$$

where the input source resistance  $R_g$  and load resistance  $R_L$  have also been included.

The two-port circuit model is also used to find the NF performance of the mixer. In this case, the resistive loss of the varactor contributes with noise both at RF and IF frequencies, which is reflected by

$$e_{nIF}^2 = e_{ni}^2 = 4kTR_s \Delta f. \quad (2.32)$$

Additionally, the resistive loss at the RF input also constitutes a source of noise which is expressed by

$$e_{n,g}^2 = 4kTR_{ip} \Delta f. \quad (2.33)$$

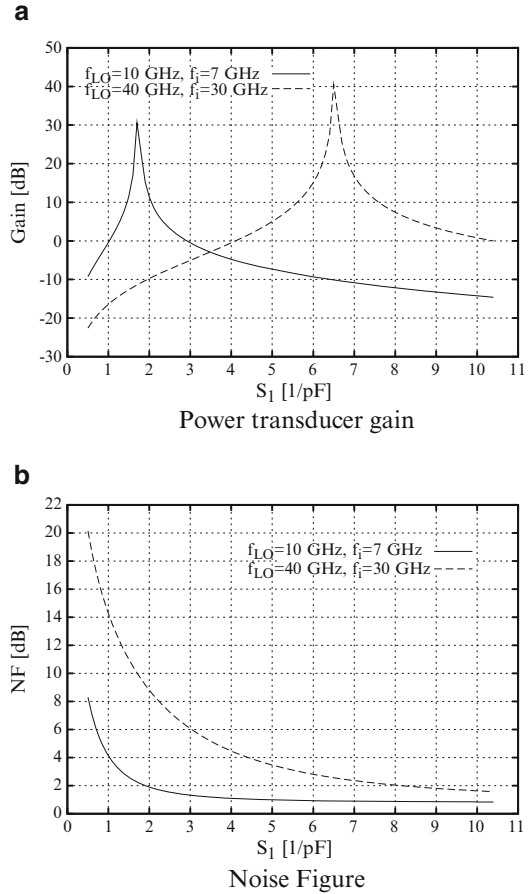
The final noise factor associated with this class of mixers is given by

$$F_{IF} = 1 + \frac{e_{ni}^2}{e_{n,s}^2} + \frac{e_{nIF}^2}{e_{n,s}^2 \cdot \left[ \frac{|S_1|}{2\pi f_i \cdot (R_{ip} + R_s)} \right]^2} \quad (2.34)$$

where it can be observed the strong dependence on the  $S_1$ , as expected.

The elastance variation range is dependent on the device but also on the pumping conditions. It has been demonstrated, [83, 86], that the elastance parameter  $S_1$  can reach up to  $10^{12} F^{-1}$  in a 130 nm CMOS with reasonable sized device and oscillator amplitude (200 mV). Based on these assumptions, the graphics represented in Fig. 2.11 trace the evolution of the transducer power gain and NF for two combinations. In the first one, it was considered a 10 GHz LO, a 7 GHz RF input signal and a 3 GHz IF. For the second case, a higher LO frequency is used (40 GHz) with an RF input of 30 GHz. It is clear from the results that  $S_1$  has to be

**Fig. 2.11** Parametric downconversion mixer gain and NF



carefully chosen in order to obtain an effective power gain higher than 1. Moreover, two possible value of  $S_1$  can reach the same gain level. The tradeoff is then made at the NF result. If a lower NF is desired, the highest  $S_1$  has to be chosen. Interestingly, it can also be observed that pushing upward the frequencies of the LO and of the input RF signals must be compensated by an increase of  $S_1$  (by changing the LO amplitude and/or the MOS varactor area).

The use of an MOS varactor as parametric mixer is still in its emerging phase. One possible implementation is the circuit is proposed in [83] which can act as the first microwave/millimeter wave frequency conversion step in a heterodyne receiver. The circuit is shown in Fig. 2.12 and includes a MOS varactor as the parametric element, two-tank, which resonate at the input/LO and idler frequencies. The input and LO signals are superimposed through the addition of the current coming from the input common gate stage, formed by  $M_1$ , and the current generated by the LO signal at  $M_2$ . The stronger LO signal will modulate the MOS varactor which is

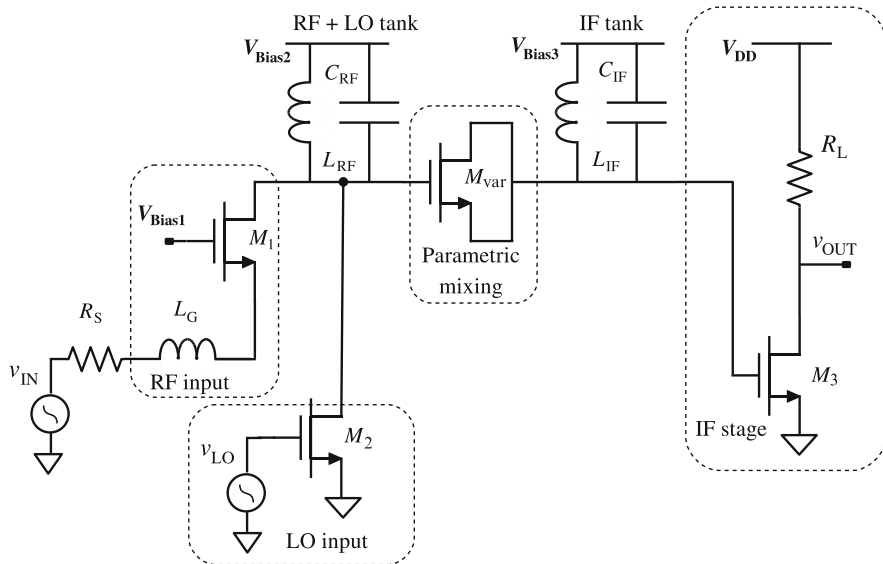


**Fig. 2.12** Simplified model of a MOSFET parametric down converter, [83]

biased by  $V_{bias2}$  and  $V_{bias3}$ . The use of the common gate input  $M_1$  ensures high bandwidth and facilitates the input  $50\ \Omega$  matching since its input impedance is roughly given by  $1/g_m$ . The mixer circuit, designed in a 130 nm technology, is able to downconvert an RF signal at 30 GHz into an IF of 10 GHz with a conversion voltage gain higher than 4 dB and a NF less than 1.8 dB. The MOS varactor is usually used as two terminal device. However, the gate-bulk capacitance can be controlled independently by a third terminal formed by the D/S connection. This three terminal MOS varactor device can be used in a discrete-time configuration as described in the next chapter. However, a continuous time operation can also be envisaged.

In complement of MOS continuous-time parametric downconverter mixer, [83, 85–88], another example is the use parametric approach in a frequency multiplier circuit [89]. The analyzed MOS mixer is to be used in a receiver chain. Nevertheless, the parametric conversion can also be very efficient in the upconversion stage of the emission chain. A first example has been proposed in a FET technology to build a Parametric MOS RF power amplifier, [90].

## 2.6 Summary

The amplification and frequency conversion based on parametric variations of reactive elements is extensive and the chapter has focused in the most important results from the supporting theory. In addition to the referred bibliography, more detailed analysis of the parametric analog signal approach can be found in [84, 91, 92].

Being the varactor the key element for the parametric approach, rather than the alternative inductor option, an overview over the varactor structures in CMOS technology was made. Of special importance is the MOS inversion mode varactor that will be the basis of the discrete-time amplification that is discussed in next chapter.

Parametric Analog Signal Amplification Applied to  
Nanoscale CMOS Technologies

Oliveira, J.; Goes, J.

2012, XXII, 186 p., Hardcover

ISBN: 978-1-4614-1670-8